Generation of the O_{630} Photointermediate of Bacteriorhodopsin Is Controlled by the State of Protonation of Several Protein Residues†

S. Bressler,‡ N. Friedman,§ Q. Li,‡ M. Ottolenghi,*,‡ C. Saha,‡ and M. Sheves*,§

Department of Physical Chemistry, The Hebrew University, Jerusalem 91904, Israel, and Department of Organic Chemistry, The Weizmann Institute of Science, Rehovot 76100, Israel

Received August 7, 1998; Revised Manuscript Received November 19, 1998

ABSTRACT: The last stages of the photocycle of the photosynthetic pigment *all-trans* bacteriorhodopsin (bR_{570}), as well as its proton pump mechanism, are markedly pH dependent. We have measured the relative amount of the accumulated O_{630} intermediate (Φ_r), as well as its rise and decay rate constants (k_r and k_d, respectively), over a wide pH range. The experiments were carried out in deionized membrane suspensions to which varying concentrations of metal cations and of large organic cations were added. The observed pH dependencies, s-shaped curves in the case of Φ_r and bell-shaped curves for k_r and k_d, are interpreted in terms of the titration of three protein residues denoted as R_1, R_2, and R_3. The R_1 titration is responsible for the increase in Φ_r, k_r, and k_d upon lowering the pH from pH ≈ 9.5 to 7. At low pH Φ_r exhibits a secondary rise which is attributed to the titration of a low pK_a group, R_2. After reaching a maximum at pH ≈ 7, k_r and k_d undergo a decrease upon decreasing the pH, which is attributed to the titration of R_3. All three titrations exhibit pK_a values which decrease upon increasing the salt concentration. As in the case of the Purple (bR_{570}) ⇔ Blue (bR_{605}) equilibrium, divalent cations are substantially more effective than monovalent cations in shifting the pK_a values. Moreover, bulky organic cations are as effective as small metal cations. It is concluded that analogously to the Purple ⇔ Blue equilibrium, the salt binding sites which control the pK_a values of R_1, R_2, and R_3 are located on, or close to, the membrane surface. Possible identifications of the three protein residues are considered. Experiments with the E204Q mutant show that the mutation has markedly affected the R_2 (Φ_r) titration, suggesting that R_2 should be identified with Glu-204 or with a group whose pK_a is affected by Glu-204. The relation between the R_1, R_2 and R_3 titrations and the proton pump mechanism is discussed. It is evident that the pH dependence of Φ_r is unrelated to the measured pK_a of the group (XH) which releases the proton to the extracellular medium during the photocycle. However, since the same residue may exhibit different pK_a values at different stages of the photocycle, it cannot be excluded that R_2 or R_3 may be identified with XH.

The photosynthetic activity of the light-driven proton pump, *all-trans* bacteriorhodopsin, bR_{570},[1] is associated with a series of spectroscopic transformations which may be represented by a simplified photocycle scheme (Scheme 1).

The arrows denote the approximate temporal order of the intermediates, while the subscripts refer to the maximum of the respective absorption bands. The various intermediates reflect structural changes both in the retinal chromophore and in the protein to which it is linked via a protonated Schiff base bond. (For a recent series of reviews on bacteriorhodopsin see ref *1*.) Accumulated evidence shows that the primary events are associated with retinal isomerization, from *all-trans* to *13-cis*, while the cross-membrane proton translocation steps occur during the later, $L_{550} \rightarrow O_{630}$, stages of the photocycle. Accordingly, the $L_{550} \rightarrow M_{412}$ transition is associated with proton transfer from the Schiff base to Asp-85, located on its extracellular side. At neutral pH this process is accompanied by proton release to the extracellular side by a group, denoted as XH, originally identified as Glu-204 (*2*). Recent work suggests that the released proton may originate from a hydrogen-bonded network of bound water molecules and acid residues (*3*). Moreover, substantial evidence indicates that also Glu-194 is involved in the release mechanism (*4, 5*). In the $M_{412} \rightarrow N_{540}$ step the Schiff base is reprotonated from Asp-96, located on the cytoplasmic side. The vectorial proton translocation is completed when Asp-96 regains a proton from the bulk during the $N_{540} \rightarrow O_{630}$ step, concurrently to *13-cis* → *all-trans* reisomerization of the chromophore. The initial state of the system is regained during the last $O_{630} \rightarrow bR_{570}$ step, as Asp-85 reprotonates the proton release group X^-. While this picture applies at neutral pH, a different sequence of proton translocation steps occurs below pH ≈ 6 which corresponds to the transient pK_a which characterizes the proton release group during the

† This research was supported by a grant from The Israel National Science Foundation, program founded by the Israel Academy of Sciences and Humanities, Centers of Excellence Program, by the U.S.−Israel Binational Science Foundation, and by the L. Farkas (HU-Minerva) Research Center.

* Author to whom correspondence should be addressed.

‡ The Hebrew University.

§ The Weizmann Institute of Science.

[1] Abbreviations: bR, bacteriorhodopsin; Purple, purple bR; Blue, blue bR; E204Q, bR mutant in which Glu-204 is replaced by glutamine; R82Q, bR mutant in which Arg-82 is replaced by glutamine; OP, 1,10-phenanthroline (*o*-phenanthroline).

10.1021/bi981901b CCC: $18.00
Published on Web 02/16/1999

Scheme 1

$$bR_{570} \xrightarrow{h\nu} H \xrightarrow{<30\ fs} I_{460} \xrightarrow{0.5\ ps} J_{625} \xrightarrow{5\ ps} K_{610} \xrightarrow{2\ \mu s} L_{550} \xrightarrow{50\ \mu s} M_{412} \xrightarrow{1\ ms} N_{540} \xrightarrow{3\ ms} O_{630} \xrightarrow{5\ ms} bR_{570}$$

photocycle (*6*). When pH < pK_a, XH does not deprotonate and proton uptake (by Asp-96) precedes proton release which is delayed until the final stage of the photocycle.

Accumulated evidence, primarily the multiexponential nature of several steps in the photocycle and their pH dependence, indicate that Scheme 1 is a rough approximation and that it should be replaced by more complex mechanisms. This problem, which is still controversial, has led to a variety of approaches based on one or on a combination of mechanistic elements such as reversible (equilibrium) steps, spectroscopically indistinguishable substates of the same intermediate, branching reactions, and the occurrence of several bR substates characterized by different protein conformations (for a recent review see ref (*7*)). Of particular interest are the photocycle stages associated with the O_{630} intermediate, which are key steps in the proton pump mechanism. An outstanding problem is to account for the observation that the relative amounts of N_{540} and O_{630} are pH dependent: O_{630} accumulates substantially below pH = 6−7, while N_{540} predominates above pH ≅ 7.5 (*8*−*12*).

Three major approaches have been proposed to account for the pH dependency of the O_{630} amplitude: (a) a (fast) pH dependent equilibration of N_{540} and O_{630} (*8*, *13*−*15*); (b) parallel formation of N_{540} and O_{630} in separate photocycles, due to a variety of pH-dependent forms of bR (*11*); (c) branching of a single photocycle into a high pH (N_{540}-accumulating branch) and a low pH (O_{630}-accumulating branch) (*12*). This mechanism correlates the pH dependency of O_{630} accumulation with the pK_a of the proton releasing group, XH.

In this study we have reexamined the pH effects on the O_{630} amplitude in bR over a concentration range of several salts. These effects were analyzed along with the effects of pH on the rates of O_{630} formation and decay. Comparative experiments were also carried out with the E204Q mutant of bR. Our purpose was to quantitatively interpret the effects in terms of the titration of specific protein residues. (For a review of acid−base equilibria in bR see ref (16).) We find that O_{630} accumulation is not simply related to the measured pK_a of the XH group. It is rather controlled by the state of protonation of at least three titrable protein residues. The nature of these residues and their relationship to the pump mechanism are discussed.

MATERIALS AND METHODS

Materials. Deionized blue membranes were obtained by passing bR suspensions through a Fluka Dowex 50Wx8 cation exchange column. Large organic cations were prepared and employed as recently described by Tan et al. (*17*). Out of the monovalent quaternary ammonium series, R_nN^+, we used the butyl derivative Bu_4N^+ Br^- (Fluka). Representative of the divalent "bolaform" series $R_3N^+-(CH_2)_n-N^+R_3B_r^-$ was the ethyl derivative, R = Et, n = 4, here denoted as $N_2Et_6C_4^{2+}$. 1,10-Phenanthroline (*o*-phenanthroline) (OP) was obtained from Aldrich. The {Fe^{2+}, 3OP} complex was prepared by mixing an $FeCl_2$ solution with 4 equiv of the corresponding ligand (*18*). The E204Q mutant of bR was received as a generous gift from Profs. R. Needleman and J. K. Lanyi.

Laser Photolysis. Membrane suspensions of native bR ([bR] ≅ 10^{-5} M) and of its E204Q mutant were exposed to 532 nm, 9 ns, pulses of a Nd:YAG laser in the presence of the background light-adapting illumination. Laser-induced absorbance changes were recorded using a continuous 75 W Xe lamp, a photomultiplier, and a TDS-520 Tektronix digitizer. Data were averaged and analyzed using a personal computer.

Procedures. Studies of salt effects on the bR photocycle were carried out by adding the required amounts of salt to the deionized (dI−bR) membrane suspensions, followed by incubation for several hours, to allow for the full Blue to Purple equilibration (*19*). The pK_a of the Blue ⇔ Purple transition for the various bR preparations was determined by recording the changes at the characteristic 630 nm maximum of the Purple ⇔ Blue difference spectrum. For this purpose spectra were recorded on a Hewlett-Packard diode-array spectrophotometer over the 2 < pH < 10 range. To ensure complete light adaptation, all experiments were carried out in the presence of background illumination (λ > 500 nm) from a 150 W halogen lamp. The pH was adjusted with NaOH/HCl.

RESULTS

As it will become evident below, in this study we were mainly interested in determining the pH dependence of the relative amount of the O_{630} intermediate below pH 6−7. There are two difficulties which have to be circumvented when studying the bR_{570} (*all-trans)* photocycle at relatively low pH. First, one must correct for the partial conversion into the blue form which is associated with the protonation of Asp-85. Second, the increasing amount of blue bR catalyzes light → dark adaptation (*25*), which represents the *all-trans* → *13-cis* isomerization reaction. Thus, to guarantee that our photolysis experiments were carried out exclusively with an *all-trans* population (*20*), we employed a continuous background light (λ > 500 nm).

A quantitative estimate of the amount of the O_{630} intermediate was obtained by defining a relative yield, Φ_r, as the ratio between the O_{630} amplitude, $\Delta D°$, and the maximum (hypothetical) amplitude of O_{630} ($\Delta D°_{max}$), attainable assuming that the initially formed M_{412} is totally converted into O_{630}. This analysis must take into consideration several factors: (a) First, at low pH, where the contribution of the blue form of bR is not negligible, one must correct for the drop in the amount of purple bR (bR_{570}). This was carried out by determining at each pH the fractions of purple and blue forms, f_p and f_b, respectively ($f_p + f_b = 1$), which are present under the steady-state background illumination conditions of our experiments. Figure 2A shows a set of such Purple ⇔ Blue titrations for a series of Na^+ amounts added to a deionized bR (dI-bR) suspension. Interestingly, at high salt concentrations, where the pk_a is shifted to lower values, the titration becomes substantially broader. This may indicate that the Purple ⇔ Blue transition is controlled by the titration

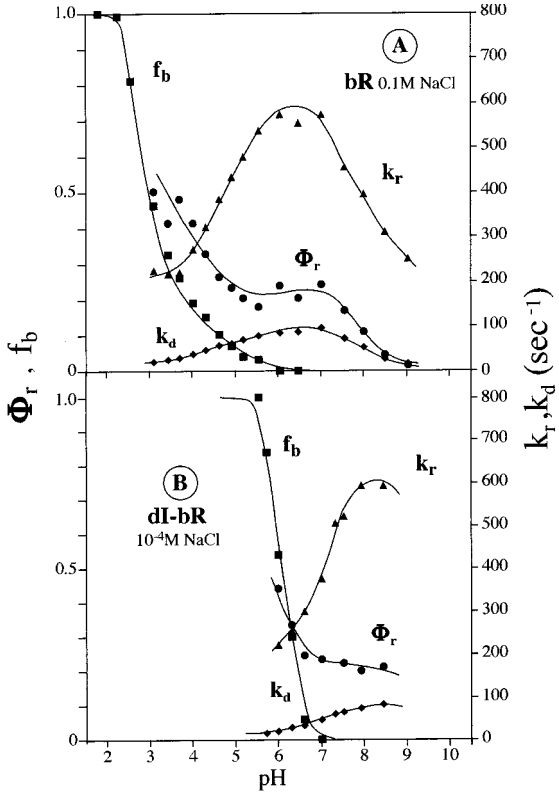

FIGURE 1: pH and salt dependence of the relative amount of the accumulated O_{630} intermediate, Φ_r, and the kinetic parameters k_r and k_d. A. A 0.1 M NaCl suspension of 10^{-5} M bR. B. A deionized, 10^{-5} M, suspension of bR, with 10^{-4} NaOH/HCl added for pH regulation ($[Na^+]/[bR] \cong 10$). Data points above pH 8.5 are not included for this low salt preparation since pH adjustment in this high-pH range requires that $[Na^+] \gg 10^{-4}$ M.

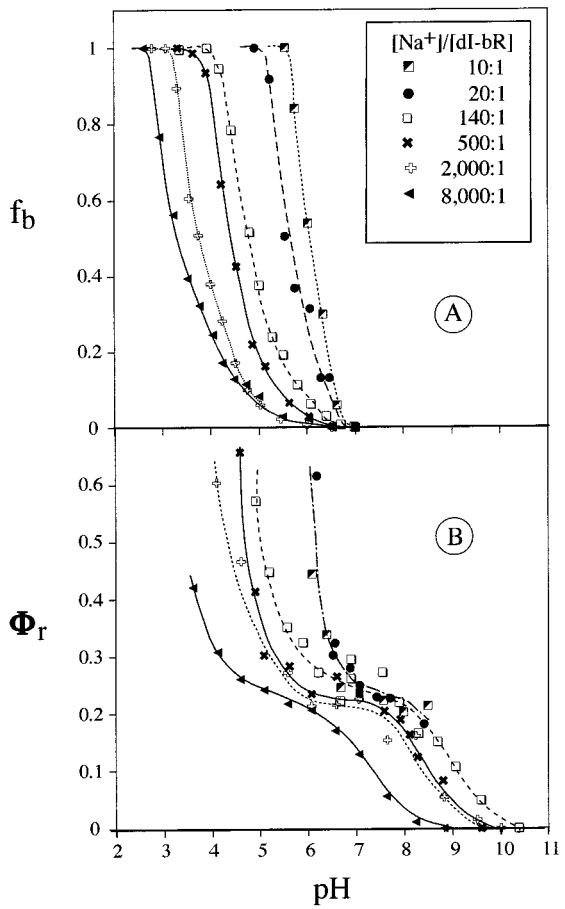

FIGURE 2: pH dependence of f_b and Φ_r for deionized bR solutions (dI-bR) to which various amounts of NaCl were added to obtain the specified $[Na^+]/[dI\text{-}bR]$ ratios. See legend to Figure 1 for the absence of data points above pH 8.5 for the lowest ratios, 10:1 and 20:1.

of more than one, e.g., two, protein residues. At low salt concentrations the pK_a values of the two titrations may coincide giving rise to a narrow titration curve. (b) Second, the photocycle of blue bR (*21*) has small, but nonnegligible, contributions at 670 nm, as well as at 412 nm (where M_{412} absorbs; see below). These contributions denoted as ΔD^b (670) and ΔD^b (412), respectively, had to be taken into account. To avoid excessive corrections for this effect, we limited our photocycle experiments to pH values which are sufficiently high to guarantee that $f_b < 0.5$. (c) Third, at the peak of its accumulation, O_{630} is still equilibrated with a small amount of the M_{412} intermediate. This contribution, denoted as $\Delta D^M{}_p$, had to be considered when calculating the maximum attainable amount of O_{630}. Thus, we have calculated Φ_r according to the expression

$$\Phi_r = \Delta D^\circ / \Delta D^\circ{}_{max}$$

where

$$\Delta D^\circ = \Delta D^\circ{}_{obs} - \Delta D^b(670) f_b$$

$$\Delta D^\circ{}_{max} = \{\Delta D^M{}_{max} 1.07 f_p - [\Delta D^M{}_p - \Delta D^b(412) f_b]\} 1.43$$

$\Delta D^\circ{}_{obs}$ is the observed absorbance change at 670 nm, and $\Delta D^M{}_{max}$ is the absorption at 412 nm, at pH 7, recorded after $\sim$250 μs, when M_{412} reaches its peak value; 1.07 is a correction factor accounting for the small superimposed contributions of L_{550} and N_{540} (*22*), and 1.43 is the differential extinction coefficient ratio: $\Delta\epsilon(O_{630}-bR_{570})/\Delta\epsilon(M_{412}-bR_{570})$. $\Delta D^M{}_{max}$ was always measured for the same solution at pH 7, since at lower pH the $L_{550} \leftrightarrow M_{412}$ equilibrium starts to be substantially shifted toward the L_{550} side (*23*). Thus, $\Delta D^M{}_{max} 1.07$ is the maximum measurable amount of the M_{412} absorbance, a value which is practically constant above pH $\approx$ 6. For $f_b < 0.5$, the contribution of the absorbance change at 412 nm, after 250 μs, due to the photocycle of the blue form, was always below 5%. It was therefore practically unnecessary to correct the first term in the $\Delta D^\circ{}_{max}$ expression for the contribution of the Blue photocycle. It should be noted that the above definition of Φ_r and its mechanistic implications are based on the assumption that O_{630} originates exclusively from M_{412}. In other words, there are no significant routes to O_{630}, branching from L_{550} or K_{610}, which circumvent M_{412}.

Figure 1A,B shows the pH dependence of the relative amount of the O_{630} intermediate for two bR preparations: (a) a purple membrane suspension, in the presence of 0.1 M NaCl; (b) an originally deionized (blue membrane) suspension with a minimum amount of NaOH (10^{-4} M, $[Na^+]/[bR] \cong 10{:}1$) required for pH regulation. In the figure we have also included the rate parameters k_r and k_d, corresponding to the rise and decay of O_{630}, respectively. Since k_r exceeds k_d by almost an order of magnitude, we have approximated the corresponding processes as non-overlapping single exponentials. In keeping with previous observa-

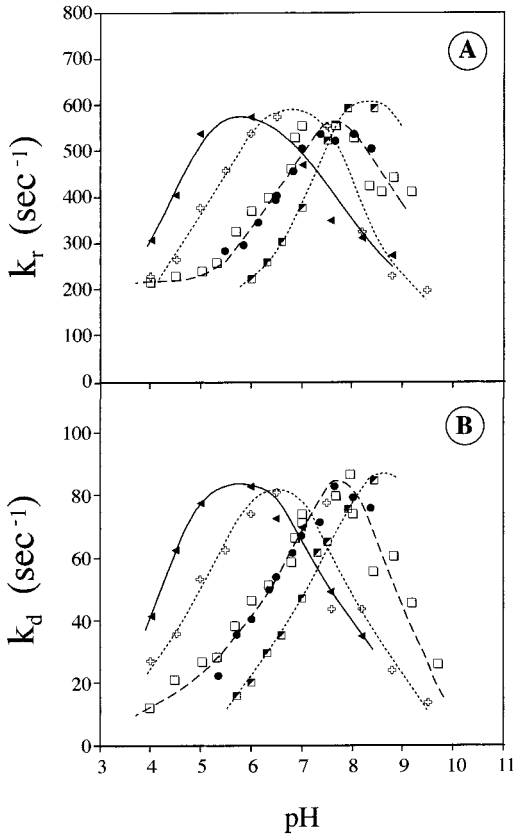

FIGURE 3: pH dependence of k_r and k_d. Same systems and notations as in Figure 2.

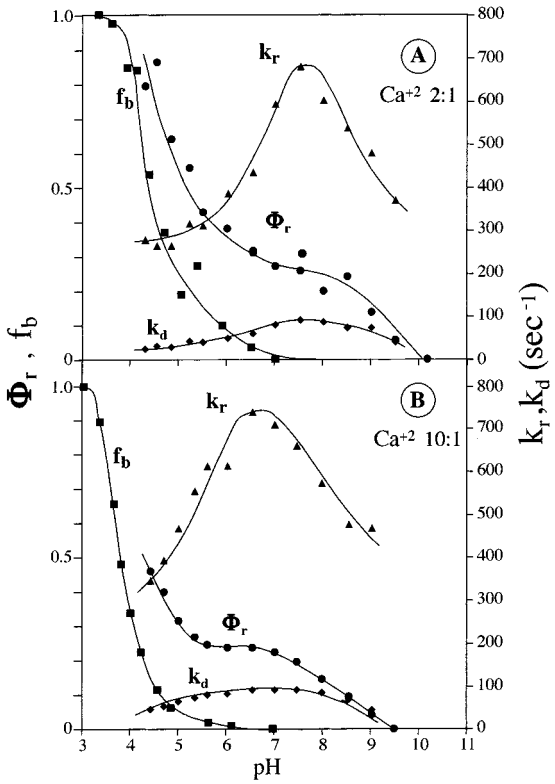

FIGURE 4: Effects of $CaCl_2$, added to the system of Figure 1B, on the pH dependence of f_b, Φ_r, k_r, and k_d. A. $[Ca^{2+}]/[bR] = 2:1$. B. $[Ca^{2+}]/[bR] = 10:1$.

tions (*8, 11, 12*) all three parameters, Φ_r, k_r, and k_d, exhibit marked drops at high pH. Figure 1 shows that additional pH effects are also observed on the low pH side. Thus, upon decreasing the pH, k_r and k_d reach a maximum value which is followed by a drop at low pH. As to the relative amount of the O_{630} intermediate, after passing through a plateau at neutral pH, Φ_r exhibits a secondary rise at low pH, reflected in the characteristic s-shaped curves.

Figure 1 indicates that both the bell-shaped curves of k_r and k_d, as well as the s-shaped curve of Φ_r, markedly depend on the salt concentration. Interpreting these curves in terms of the superimposed titrations of various protein residues, the observed salt effects are accounted for, in terms of the sensitivity of the pK_a values of such titrations to the salt concentration (see discussion below). A more quantitative dependence on salt concentration was obtained by adding controlled amounts of various salts to the deionized (dI-bR) preparation. Figures 2 and 3 show the effect of added NaCl on the amplitude parameters f_b, Φ_r, and k_r, k_d, respectively, for several $[Na^+]/[bR]$ ratios. Figure 4 shows the effect of added Ca^{2+} for the two $[Ca^{2+}]/[bR]$ ratios, 2:1 and 10:1.

It is evident from Figures 1−4 that the various components of the titration-like curves of k_r, k_d, and Φ_r show a general dependence on salt which is analogous to that of f_b. Namely, the corresponding titration-like curves shift to lower pH values at higher salt concentrations, with the bivalent Ca^{2+} cation being more effective, by almost 2 orders of magnitude, than Na^+. (For a review of metal ions binding to bR and their effect on the Purple ⇔ Blue transition see ref (*24*).) An additional characteristic of the Purple ⇔ Blue equilibrium in bR is the observation (*17, 18*) that the purple form may also be regenerated from blue dI-bR preparations by the addition of large organic cations. We have therefore extended our measurements to the monovalent quaternary butylammonium ion Bu_4N^+, to the divalent "bolaform" cation $Et_3N^+-(CH_2)_4-N^+Et_3$ ($N_2Et_6C_4^{2+}$), and to the large cationic complex formed between Fe^{2+} and 1,10-phenanthroline (OP), $\{Fe^{2+}, 3OP\}$. Characteristic data are presented in Figure 5 and in Table 1.

As outlined above an analogy was proposed between the pK_a of the proton release group, XH, and the apparent pK_a of O_{630} formation (*7, 12*). Since proton release is abolished when Glu-204 is replaced by glutamine (*2*), it seems relevant to investigate the pH dependence of O_{630} accumulation in the E204Q mutant of bR. The corresponding pH effects are given in Figure 6 for both Φ_r and the kinetic parameters k_r and k_d. In keeping with the recent investigation of Misra et al. (*15*), k_r and k_d exhibit an increase upon lowering the pH from pH ≈ l0 to pH ≈ 7 which is qualitatively analogous to that of the native system. We note, however, that the maximum value of Φ_r obtained for E204Q at pH ≈ 6.8 is higher than the corresponding plateau in the native system (see, e.g., Figure 1A). The corresponding value, $\Phi_r \approx 0.6$, is obtained in native bR only after a substantial contribution of the second pH effect at pH ≈ 4. An additional difference between the native pigment and E204Q is the less pronounced drop of k_r and the pH independency of k_d at low pH. However, the most dramatic effect of the mutation is the inversion of the low pH effect on Φ_r. Thus, in the case of E204Q, after reaching the maximum at pH ≈ 6.8, further decrease in pH causes a decrease rather than an increase in O_{630} accumulation.

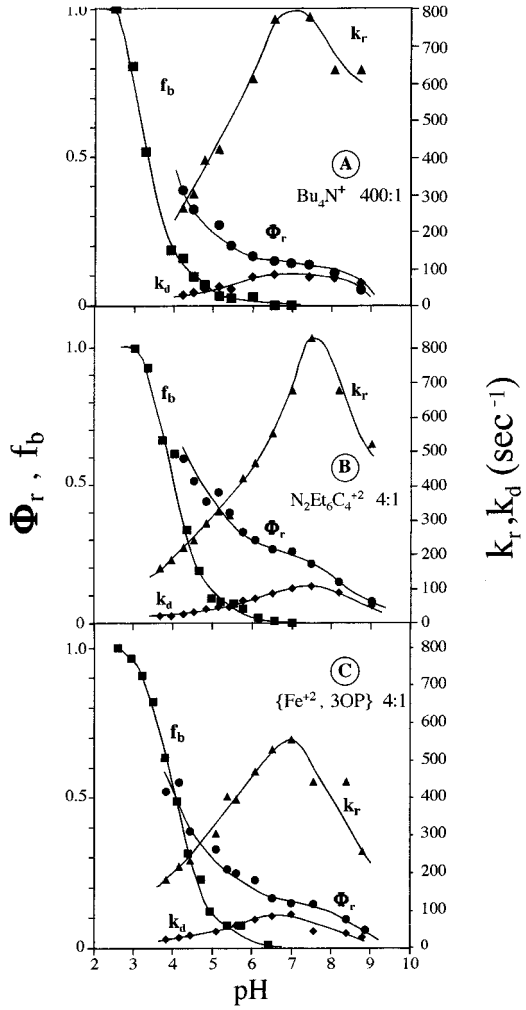

FIGURE 5: Effects of large organic ions and of a metal organic ionic complex, added to the system of Figure 1B, on the pH dependence of f_b, Φ_r, k_r, and k_d.

DISCUSSION

Interpretation of pH Effects in Terms of Several Titrable Protein Residues. Our major objective is to interpret the pH-dependence of the amplitude and kinetics of the O_{630} intermediate in terms of the titration of specific protein residues. (See ref (*16*), for a general discussion of acid−base equilibria in bacteriorhodopsin.) It is evident that the titration-like curves of Figures 1−6 cannot be assigned to a single titration. The simplest approach would be to interpret the data in terms of two protein residues, R_1 and R_2, which may be titrable independently or may be coupled according to the model of Balashov et al. (*25*) which was applied to the Purple ⇔ Blue transition. Considering for example an amplitude (Φ_r) curve such as in Figure 1A, the respective pK_a values will correspond to the apparent values pK_a(1) ≈ 8 and pK_a(2) > 3.3, where (1) and (2) refer to the high and low pK_a titrations, respectively. It is important to emphasize that the above pK_a values, as well as the other reported in this work (see discussion below), are qualitative estimates. An accurate analysis (as, e.g., in ref (*18*)) was precluded in the case of k_r and k_d by the lack of accurate values of these parameters at both highest and lowest ends of the bell-shaped curves. Moreover, the value assigned to pK_a(2) is only a lower limit. This stems from the fact that, due to the transition to the blue form and the implied corrections, the titrations cannot be completed at their lowest pH end.

Nevertheless, an analysis of the bell-shaped and s-shaped curves in terms of several superimposed titrations, allows us to derive some basic conclusions. For example, a closer examination of the data reveals that the titration of the two protein residues, (1) and (2), is not sufficient for accounting for *both* amplitude and kinetic curves. As shown in Table 1, a comparison of the Φ_r titrations with the corresponding titrations of k_r and k_d shows a similar apparent pK_a value for the first, high pH, titration of the three parameters. However, in many cases the low pH range of the bell-shaped curves of k_r and k_d, denoted as titration (3), exhibits an apparent pK_a which is unambiguously higher than that [pK_a(2)] estimated for the lowest pH region of the Φ_r curves. For example, in the case of the 10:1 [Na^+]/[bR] system (Figure 1B), the onset of titration (2) is observed at pH ≈ 6.5 where the k_r titration is essentially completed. We therefore suggest that both amplitude and kinetic titrations in the high pH are associated with the same residue (1), but that different moieties, R_2 and R_3, are responsible for the low-pH region of the Φ_r titration and for the low pH side of the bell-shaped kinetic titrations, respectively. The conclusion that the same titrations, (1) and (3), are responsible for the bell-shaped curves of both k_r and k_d is further demonstrated by the fact that the two parameters reach their maximum value at the same pH, pH_{max} (see Table 1).

Dependence of the Apparent pK_a Values on the Type and Concentration of Metal Ions: Comparison with the Purple ⇔ Blue Transition. It is clearly evident from Figures 1−6 that the apparent pH titrations of both amplitude and kinetic parameters associated with the O_{630} intermediate, are all highly sensitive to the amount and type of the salts. Salt effects on pK_a(1), pK_a(2), and pK_a(3) are summarized in Table 1, where they are compared with those related to the Purple ⇔ Blue equilibrium of the unphotolyzed pigment, which is the best understood titration of a protein residue in bR (*16*). The Purple to Blue transition, which is associated with the protonation of Asp-85, can be induced by acidification as well as by deionization. Thus, it has long been recognized that the apparent pK_a of the titration of Asp-85 depends on salt concentration (for a review, see ref (*24*)). The detailed way by which the titration is affected by salts is not exactly understood. However, accumulated evidence points out that two mechanisms play a major role in determining the way by which cations control the apparent pK_a of Asp-85: (a) The binding of metal cations at two specific (high affinity) sites, which induces a reduction in the pK_a of Asp-85 (*17*, *26*−*29*). This mechanism seems to be important at very low salt concentrations. (b) At higher salt concentrations the predominant mechanism appears to be associated with nonspecific effects of the cations on the surface potential of the bR membrane which decrease the local proton concentration and thus the pK_a of the titration (*30*−*35*). Independently of the specific mechanism it was established that the binding constants, and thus the effects on pK_a (P ⇔ B), of divalent cations such as Ca^{2+} and Mg^{2+} are almost 2 orders of magnitude larger than those of e.g., Na^+ and K^+. Recently it was observed that the metal cations can be effectively replaced by large organic cations, such as the monovalent R_4N^+ and the divalent 'bolaform' $N_2R_6C_n^{2+}$ cations (*17*), as well as by the even larger transition metal

Table 1: pH and Salt Effects on the Purple ↔ Blue (P ⇔ B) Equilibrium and on the Φ_r, k_r, and k_d Parameters Associated with the O_{630} Intermediate

		P ↔ B	Φ_r		k_r			k_d		
salt	$[M^{n+}]/[bR]$	pK_a	pK_a(1)	pK_a(2)	pK_a(1)	pK_a(3)	pH$_{(max)}$	pK_a(1)	pK_a(3)	pH$_{(max)}$
NaCl[b]	0.1 M	3.2	8.1	>3.1[d]	7.9	4.6	6.4	8.0	4.6	6.6
	10:1	6.1		>5.9		7.1	8.5		6.9	8.5
	20:1	5.7		>5.9		6.5	7.7		6.5	7.7
	140:1	4.8	9.2	>4.8	8.3	6.5	7.5	9.2	6.5	7.8
	500:1	4.4	8.4	>4.5	8.3	5.2	7.0	8.4	5.3	7.2
	2000:1	3.8	8.2	>3.9	8.2	5.0	6.5	8.2	4.8	6.6
	4000:1	3.5	8.2	>3.6	7.7	4.6	6.3	7.9	4.4	6.2
	8000:1	3.3	7.2	>3.3	7.2	4.5	5.7	7.3	4.4	5.8
$CaCl_2$[c]	2:1	4.4	8.9	>4.7	8.9	6.6	7.6	9.1	6.4	7.7
	10:1	3.8	8.3	>3.9	8.1	5.3	6.7	8.3	5.1	6.8
Bu_4NBr[c]	200:1	4.1	8.4	>4.3	8.4	5.9	7.5	8.4	6.0	7.5
	400:1	3.4	8.3	>3.6	8.2	5.5	7.0	8.2	5.4	7.0
$[N_2Et_6C_4]Br_2$[c]	4:1	4.1	8.4	>3.9	8.3	6.7	7.6	8.4	6.6	7.5
	80:1	3.4	7.9	>3.6	7.8	5.2	6.5	7.8	5.2	6.5
$\{Fe^{2+},3OP\}Cl_2$[c]	4:1	4.1	8.2	>4.1	8.3	5.8	7.0	8.2	5.8	7.0
	8:1	3.6	7.9	>3.7	7.8	5.6	6.5	7.9	5.4	6.5

[a] The table presents the apparent pK_a values of the three titrations attributed to R_1, R_2, and R_3, as well as the pH [pH$_{(max)}$] corresponding to the maximum values of the k_r and k_d. [b] Non-deionized bR preparations to which the reported amount of salt was added. [c] Deionized bR preparations with 10:1 Na^+ to which the reported amount of salt was added. [d] The values reported are lower limits of pK_a(2), estimated by assuming that on the low pH side of the titration, Φ_r ultimately reaches its maximum value, $\Phi_{r(max)} = 1$. Actual pK_a values may be higher, if $\Phi_{r(max)} < 1$.

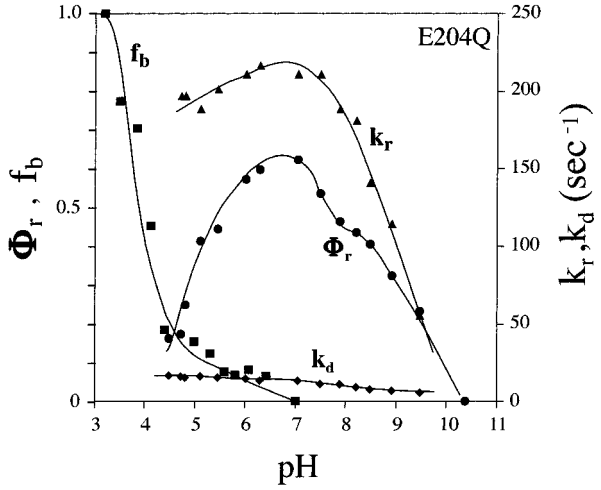

FIGURE 6: pH dependence of f_b, Φ_r, k_r, and k_d in the case of E204Q (0.01 M NaCl).

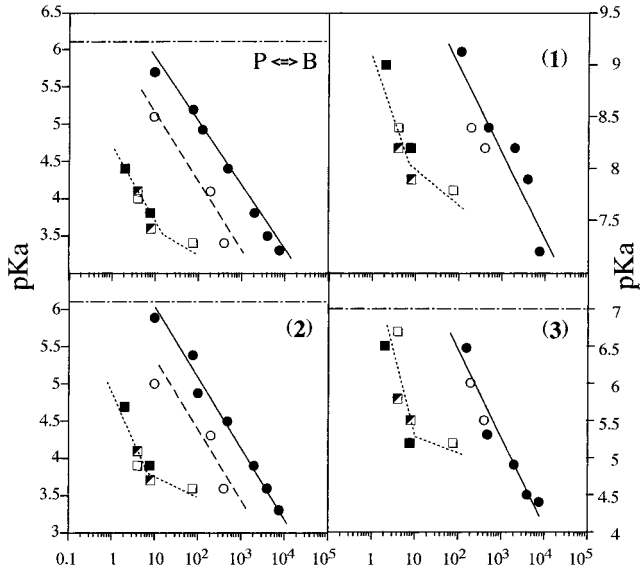

FIGURE 7: Plots of the pK_a values of the P ⇔ B transition and of the photocycle parameters Φ_r, k_r, and k_d, presented in Table 1, versus the concentration of the various cations. (1), (2), and (3) denote the three titrations as described in the text. pK_a(1) and pK_a(3) values are an average of those measured for Φ_r, k_r, and k_d and for k_r, and k_d, respectively. The horizontal broken lines denote the pK_a value of each titration in the low $[Na^+]$ system of Figure 1B. Note that in the case of pK_a(2) the figures represent a lower limit (see text and Table 1). Salt notations: ●, Na^+; ○, Bu_4N^+; □, $N_2Et_6C_4^{2+}$; ■, Ca^{2+}, ◩, $\{Fe^{2+}, 3OP\}$.

complex $\{Fe^{2+}, 3OP\}$ (*18*). These observations, especially the study of the kinetics of the Purple⇔Blue transition, led to the conclusion that the high affinity cation binding sites which control the titration of Asp-85 are in an exposed location, on the membrane surface or close to it (*18*).

A comparison of the salt effects on the titrations of R_1, R_2, and R_3 with those of the Purple ⇔ Blue transition is best visualized by means of Figure 7, in which the pK_a values of the four titrations are plotted versus the $[M^{+2}]/[bR]$ ratio for the various cations employed. Two principal features and related conclusions are evident: (a) In all cases the large organic cations are as effective as the small metal cations of the same valency in shifting the respective pK_a values. (b) The bivalent cations are always substantially more effective in shifting the pK_a than the monovalent cations. *It therefore appears that the cation-binding protein residues which control the titrations of R_1, R_2, and R_3 are located on, or close to, the membrane surface.* (This conclusion does not exclude the possibility that the cations bind directly to R_1, R_2 and R_3, thus affecting their pK_a values.) Moreover, since both features a and b also characterize the Purple ⇔ Blue titration, it seems that the same surface residues control the titration of Asp-85 in the unphotolyzed pigment and the yield and kinetics of O_{630} during the photocycle.

On the Nature of the Protein Residues Which Control the Accumulation and Kinetics of the O_{630} Intermediate. Although a clear identification of residues R_1, R_2, and R_3 is still unavailable, it is tempting to consider several feasible assignments of these moieties. The most relevant clues are

provided by the effects of the glutamine replacement of the Glu-204 residue, which appears to play a key role in the proton pump mechanism. As shown in Figure 6, and in keeping with the observations of Misra et al. (*15*), the pH dependence of k_r for this mutant shows a bell-shaped behavior which is similar to that of native bR, though with a much less pronounced drop on the low-pH side. The latter is essentially absent in the case of the k_d titration. It therefore appears that the kinetic effects associated with the R_3 titration are substantially attenuated by the replacement of Glu-204 by glutamine. More substantial differences between the Glu-204 mutant and native bR are observed for the Φ_r titration. In the case of E204Q, Φ_r exhibits a rise from pH $\approx$ 10 to 6, which is qualitatively analogous to that of native bR. However, a completely different behavior is observed on the low-pH side, where the upward R_2 titration of the native system is replaced by a sharp drop. Moreover, in the case of E204Q the maximum Φ_r value at pH 7 is as high as that attained in the native system only at lower pH, after a substantial contribution of the R_2 titration. We interpret these observations by identifying R_2 with Glu-204, or with a residue whose pK_a is affected by Glu-204. According to this interpretation the Glu-204 $\rightarrow$ glutamine mutation has not substantially affected the high pH, pK_a(1), titrations of Φ_r, k_r and k_d. It has attenuated the drops at low pH in the pK_a(3) titration of k_r, and k_d, but it has completely eliminated the low-pH pK_a(2) effect, revealing an additional titration of a residue (denoted as R_4) which is responsible for the marked drop of Φ_r at low pH. Interestingly, the E74C mutation of the neighboring Glu-74 residue does not induce substantial changes in the pH patterns of Φ_r , k_r, and k_d, with respect to those of the native pigment (unpublished work in this laboratory).

When considering the identity of R_2 it is also relevant to recall that in the case of E204Q the maximum value of Φ_r is considerably higher and the range of the high-pH effect on Φ_r is broader, with respect to native bR. This may suggest that rather than eliminating the R_2 titration, the mutation has shifted the titration to high pH, so that in E204Q it extensively overlaps with that of R_1. In fact, the high pH effect on Φ_r in E204Q may be indicative of two titrations with pK_a $\cong$ 7.5 and pK_a $\cong$ 9.0, respectively. Obviously, according to this interpretation, R_2 cannot be identified with Glu-204, but rather with a group whose pK_a is affected by Glu-204. In such a case a plausible candidate for R_2 may be Glu-194 which along with Glu-204 is part of the proton releasing complex (*4*, *5*). One should also consider the identity of residue R_4 (pK_a $\cong$ 5 in E204Q) whose titration effects are revealed in the pH dependence of Φ_r in E204Q. Such a titration may also occur in native bR, but in this case the drop in Φ_r induced by the protonation of R_4 should be more than compensated for by the R_2 titration. Alternatively, in the case of the native pigment the R_4 titration may take place in a lower pH range, shifting to higher pH upon E204Q mutation. At present we cannot identify R_4 but do not exclude the possibility that R_4 and R_3 (see below) represent the same protein residue.

It is difficult to suggest a clear identification of the intermediate and high pK_a groups, R_3 and R_1. R_3 appears to be affected by the Glu-204 mutation, so that, if R_2 is Glu-204, R_3 may be identified with Glu-194. As to R_1, it is tempting to compare the high-pH R_1 titration of the O_{630} intermediate with that observed in the case of a red shifted O-like intermediate (O_l) in the photocycles of *13-cis* bR analogues (*36*). O_l is equilibrated with a blue-shifted (L- or N-like) species, exhibiting a pK_a of about 9, which was attributed to the titration of Asp-85. Accordingly, the pK_a of this group has increased from $\sim$3.7 in the unphotolyzed form, to $\sim$8 during the O_l stage of the photocycle. However, in the present case the identification of R_1 as Asp-85 is probably unacceptable since it contradicts FTIR studies (*14*, *37*), showing that during the later stages of the photocycle, Asp-85 retains its protonated form even at the high pH values which are beyond the R_1 titration. Another possibility is to identify R_1 with Arg-82. In fact, in mutants such as R82Q or R82A, which lack the protonable arginine residue, O_{630} accumulates only at relatively high temperatures (*12*). It may thus be relevant to study the pH effects in the above mutants under high-temperature conditions. It should finally be noted that the R_1 titration may be related to the proton translocation mechanism. Thus, it was suggested that the efficiency of the proton pump is fully (*8*) or partially (*9*) affected by the R_1 titration. Similarly the "B2" component of the photocurrent in bR membrane layers, which is indicative of proton translocation, exhibits a titration-like curve with an apparent pK_a $\approx$ 8.0 (*38*), which is close to that of R_1. Since in the R82Q and R82A mutants the initial proton release is delayed until the end of photocycle (*39*), these observations may support the identification of R_1 as Arg-82.

We finally consider the relation between the measured pK_a of the proton releasing group (XH) and those of R_1, R_2, and R_3. Since none of the latter coincides with that measured for XH [pK_a(XH) = 5.8 in 0.1 NaCl(6)], we conclude that the accumulation of O_{630} is not simply related to the state of protonation of XH. One should recall, however, that the pK_a of XH is determined at the photocycle stage in which the proton is released (the $L_{550} \rightarrow M_{412}$ stage), while that of R_3 corresponds to the later $M_{412} \rightarrow O_{630}$ stage. Since pK_a(XH) may decrease after the formation of M_{412}, it cannot be excluded that XH may be identified with R_2 or R_3. Such identity is in keeping with the evidence (*2*−*5*) suggesting that XH represents a hydrogen-bonded complex involving Glu-194 and Glu-204, and with the observation that the titrations of R_2, R_3, and XH are all affected by the Glu-204 mutation. Future studies will be required to analyze the feasibility of such an identity.

NOTE ADDED IN PROOF

Preliminary experiments with the R82Q mutant at high temperature reveal the R_1 titration in the same pH range as in native bR. On the other hand, in D96N, in the presence of azide, the R_1 titration is markedly shifted. This excludes the identification of R_1 as R82, suggesting that this, high pK_a, titration may be associated with D96 or with a group whose pK_a is affected by D96.

REFERENCES

1. Ottolenghi, M., and Sheves, M., Eds. (1995) The Photophysics and Photochemistry of Retinal Proteins, *Isr. J. Chem. 35*, 193−513.
2. Brown, L. S., Sasaki, J., Kandori, H., Maeda, A., Needleman, R., and Lanyi, J. K. (1995) *J. Biol. Chem. 270*, 27122−27126.
3. Rammesberg, R., Huhn, G., Lübben, M., and Gerwert, K. (1998) *Biochemistry 37*, 5001−5009.

4. Balashov, S., Imasheva, E., Ebrey, T., Shen, N. Menick, D., and Crouch, R. (1997) *Biochemistry 36*, 8671−8676.
5. Dioumaev, A. K., Richter, H.-T., Brown, L. S., Tanio, M., Tuzi, S., Saito, H., Kimura, Y., Needleman, R., and Lanyi, J. K. (1998) *Biochemistry 37*, 2496−2506.
6. Zimanyi, L., Váró, G., Chang, M., Ni, B., Needleman, R., and Lanyi, J. K. (1992) *Biochemistry 31*, 8535−8543.
7. Lanyi, J. K., and Váró, G. (1995) *Isr. J. Chem. 35*, 365−386.
8. Lozier, R. H., Niederberger, W., Ottolenghi, M., Sivorinovksy, G., and Stoeckenius, W. (1978) in *Energetics and Structure of Halophilic Microoganisms*, Caplan, S. R., and Ginzburg, M., Eds., pp 123−139, Elsevier/North-Holland, Amsterdam.
9. Li, Q., Govindjee, R., and Ebrey, T. G. (1984) *Proc. Natl. Acad. Sci. U.S.A. 81*, 7079−7082.
10. Ames, J. B., and Mathies, R. A. (1990) *Biochemistry 29*, 7181−7190.
11. Eisfeld, W., Pusch, C., Diller, R., Lohrmann, R., and Stockburger, M. (1993) *Biochemistry 32*, 7196−7215.
12. Cao, Y., Brown, L. S., Needleman, R., and Lanyi, J. K. (1993) *Biochemistry 32*, 10239−10248.
13. Chernavskii, D. S., Chizhov, I. V., Lozier, R. H., Murima, T. M., Prochorov, A. M., and Zubov, B. V. (1989) *Photochem. Photobiol. 49*, 649−653.
14. Souvignier, G., and Gerwert, K. (1992) *Biophys. J. 63*, 1393−1405.
15. Misra, S., Govindjee, R., Ebrey, T. G., Chen, N., Ma, J.-X., and Crouch, R. K. (1997) *Biochemistry 36*, 4875−4883.
16. Honig, B., Ottolenghi, M., and Sheves, M. (1995) *Isr. J. Chem. 35*, 429−446.
17. Tan, E. H. L., Govender, D. S. K., and Birge, R. R. (1996) *J. Am. Chem. Soc. 118*, 2752−2753.
18. Fu, X., Bressler, S., Ottolenghi, M., Eliash, T., Friedman, N., and Sheves, M. (1997) *FEBS Lett. 416*, 167−170.
19. Friedman, N., Rousso, I., Sheves, M., Fu, X., Bressler, S., Druckmann, S., and Ottolenghi, M. (1997) *Biochemistry 36*, 11369−11380.
20. Balashov, S., Imasheva, E., Govindjee, R., Sheves, M., and Ebrey, T. (1996) *Biophys. J. 71*, 1973−1984.
21. Mowery, P. C., Lozier, H., Chae, Q., Tseng, T. W., Taylor, M., and Stoeckenius, W. (1979) *Biochemistry 18*, 4100−4107. Váro, G., and Lanyi, J. K. (1989) *Biophys. J. 56*, 1143−1150.
22. Váró, G., and Lanyi, J. K. (1991) *Biochemistry 30*, 5008−5015.
23. Zimányi, L., Váró, G., Chang, M., Ni, B. Needleman, R., and Lanyi, J. K. (1992) *Biochemistry 31*, 8535−8543.
24. El-Sayed, M. A., Yang, D., Yoo, S.-K., and Zhang, N. (1995) *Isr. J. Chem. 35*, 465- 474.
25. Balashov, S. P., Govindjee, R. Imasheva, S., Misra, S., Ebrey, T. G., Feng, Y., Crouch, R. K., and Menick, D. R. (1995) *Biochemistry 34*, 8820−8834. Balashov, S. P., Imasheva, E. S., Govindgee, R., and Ebrey, T. G. (1996) *Biophys. J. 70*, 473−481.
26. Ariki, M., and Lanyi, J. K. (1986) *J. Biol. Chem. 261*, 8164−8174
27. Jonas, R., and Ebrey, T. G. (1991) *Proc. Natl. Acad. Sci. U.S.A. 88*, 149−153.
28. Kimura, Y., Ikegami, A., and Stoeckenius, W. (1984) *Photochem. Photobiol. 40*, 641−646.
29. Ariki, M., Magde, D., and Lanyi, J. K. (1987) *J. Biol. Chem. 262*, 4947−4951.
30. Concoran, T. C., Ismail, K. Z., and El-Sayed, M. A. (1987) *Proc. Natl. Acad. Sci. U.S.A. 84*, 4094−4098.
31. Dunach, M. Seigneuret, M., Rigaud, J. L., and Padros, E. (1987) *Biochemistry 26*, 1179−1186.
32. Szundi, I., and Stoeckenius, W. (1988) *Proc. Natl. Acad. Sci. U.S.A. 84*, 3681−3684.
33. Gat, Y., Friedman, N., Sheves, M., and Ottolenghi, M. (1997) *Biochemistry 36*, 4135−4148
34. Braiman, M., Magi, T., Marti, T., Stern, L., Khorana, H. G., and Rothschild, K. (1998) *Biochemistry* 27, 8516−8520. Fahmy, K., Weidlich, O., Engelhard, M., Fitter, J., Oesterhelt, D., and Siebert, F. (1992) *Photochem. Photobiol. 56*, 1073−1083. Pfefferle, J., Maeda, A., Sasaki, J., Yoshizawa, T. (1991) *Biochemistry 30*, 6548−6556. Braiman, M., Bousche, O., and Rothschild, K. (1991) *Proc. Natl. Acad. Sci. U.S.A. 88*, 2388−2392. Hessling, B., Souvignier, G., and Gerwert, K. (1993) *Biophys. J. 65*, 1929−1941.
35. Kono, M., Misra, S., and Ebrey, T. (1993) *FEBS Lett. 331*, 31−37.
36. Balashov, S., Govindjee, R., Kono, M., Imasheva, E., Lukashev, E., Ebrey, T., Crouch, R., Menick, D., and Feng, Y. (1993) *Biochemistry 32*, 10331−10343.

BI981901B